UCRL-JC-127877
PREPRINT

First-Principles Study of High Explosive Decomposition Energetics

C.J. Wu
L.E. Fried

This paper was prepared for submittal to the
Eleventh International Detonation (1998) Symposium
Snowmass, CO
Aug. 31- Sept. 4, 1998

August 21, 1998

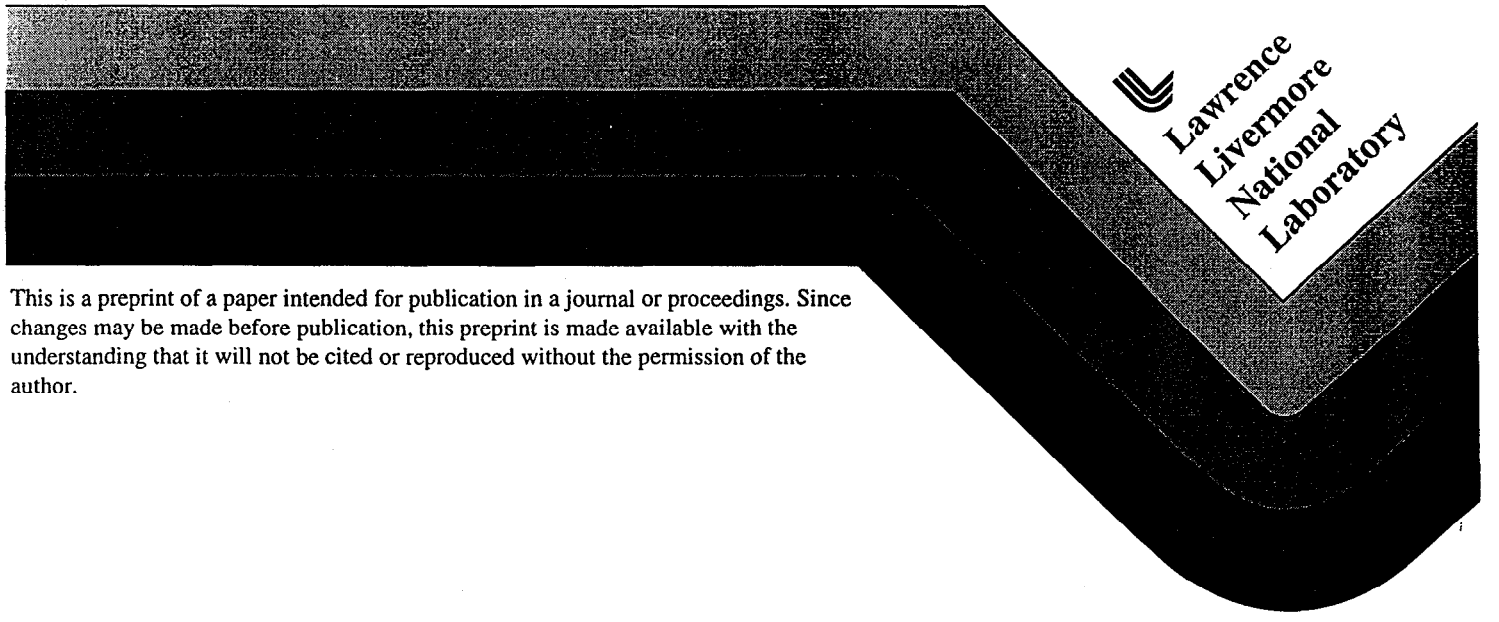

FIRST-PRINCIPLES STUDY OF HIGH EXPLOSIVE DECOMPOSITION ENERGETICS

C. J. Wu and L. E. Fried
Lawrence Livermore National Laboratory
Livermore, CA 94550

The mechanism of the gas phase unimolecular decomposition of hexahydro-1,3,5,-trinitro-1,3,5,-triazine (RDX) has been investigated using first principles gradient corrected density functional theory. Our results show that the dominant reaction channel is the N-NO_2 bond rupture, which has a barrier of 34.2 kcal/mol at the B-PW91/cc-pVDZ level and is 18.3 kcal/mol lower than that of the concerted ring fission to three methylenenitramine molecules. In addition, we have carried out a systematic study of homolytic bond dissociation energies of 14 other high explosives at the B-PW91/D95V level. We find that the correlation between the weakest bond strength and high explosive sensitivity is strong

INTRODUCTION

The molecular decomposition of high explosives has been regarded as an important step in explosive detonation kinetics. In particularly, the dissociation energy of the weakest bond of the explosive molecule is likely to play an important role in initiation events. However, this essential chemical property has not been determined for many high explosives. A systematic study of this quantity should be useful in understanding initiation chemistry.

The first system that we have chosen to study is a widely used high explosive and monopropellant, hexahydro-1,3,5,-trinitro-1,3,5,-triazine (RDX). Although it is one of the most thoroughly studied energetic compounds, even simple questions such as the nature of the initial step in the thermal decomposition of RDX are still a subject of debate.

There are many suggested initial unimolecular steps in the thermal decomposition of RDX. Among them, the most supported mechanisms are (I) N-NO_2 bond rupture, and (II) concerted ring fission to three $CH_2N_2O_2$. For instance, a recent supporting evidence for path I was given by the transient IR laser pyrolysis experiments of Wight and Botcher.[1] Using a solid RDX thin film, they found that the initial decomposition products relate mostly to the N-NO_2 bond rupture. In addition, their experiments on samples with isotopically labeled nitrogen also showed that decomposition of RDX is mostly unimolecular and involves the removal of only one NO_2. On the other hand, there is also experimental evidence for path II. Using infrared multiphoton dissociation (IRMPD) of RDX in a molecular beam, Zhao, Hintsa and Lee found that a branching ratio of 2:1 for the path II over the path I best matched their time of flight spectra. Therefore, they concluded that the dominant channel is the symmetric ring-fission II, not the N-NO_2 bond cleavage I.

The disagreement on the mechanism may be attributed to differing experimental conditions. It has been postulated that the solid and liquid confining environment may prohibit the ring fission reaction from proceeding. Since gas phase molecular theory provides a direct comparison to collision-free molecular beam experiments, it can be used to help determine whether the disagreement is due to experimental conditions.

Several theoretical studies related to gas phase RDX decomposition have been reported. Melius and Binkley have estimated the N-NO_2 bond dissociation energy to be about 48 kcal/mol based on the assumption that RDX has a N-NO_2 bond dissociation energy similar to that of nitramine and methyl-nitramine. The barrier of 72.2 kcal/mol for the ring-fission II was previously predicted by Habibollahzadeh et. al. using the local density functional procedure with a Hartree-Fock (HF) optimized (STO-3G basis set) geometry. Nevertheless, the local density approximation (LDA) employed by Habibollahzadeh et. al. has recently been shown to be unreliable for predicting barrier heights.

The deficiencies of LDA in predicting molecular thermochemistry have been significantly overcome by recently developed gradient-corrected functionals in generalized gradient approximations (GGA). Roughly speaking, GGA gives much better results than LDA, and in many cases it provides a level of accuracy similar to other

sophisticated *ab initio* methods. In addition, density functional theory (DFT) methods scale much better with the system size (order N^3, where N is the number of basis functions) than high level quantum methods of similar accuracy or greater (order N^5 or more), therefore they are particularly suitable for the study of large systems such as RDX.

In the first part of this paper, we present a detailed study of RDX unimolecular dissociation via path I and II using state-of-art first-principles gradient-corrected DFT methods in order to clarify previous work. A range of basis sets and modern gradient corrected density functional methods were applied to this problem, in order to ensure that the final conclusion does not depend on computational methods.

Once we determined the minimum basis set and the functional for reliably predicting bond dissociation energy, we apply them to calculate bond dissociation energies of 11 common high explosive molecules ranging from highly sensitive (e.g. Nitroglycerin) to insensitive ones (e.g. TATB). The first six high explosive molecules are nitrated aromatic benzene rings: 1,3,5-Triamino-2,4,6-trinitrobenzene (TATB), 1,3-diamino-2,4,6-trinitrobenzene (DATB), 1-amino-2,4,6-trinitrobenzene (MATB), 2,4,6-trinitrobenzene (TNB), 2,4,6-trinitrotoluene (TNT) and hexanitrobenzene (HNB). We also have molecules that are saturated cyclic nitramines: 1,3,5,7-tetramethylene-2,4,6,8-tetranitramine (HMX); and RDX. In addition, we included TNAZ, NTO, EDNA, DINGU, pentaerythritol tetranitrate (PETN), Nitroglycerin and tetryl.

In the second part of this paper, we report possible homolysis bond strengths for each high explosive and identified the weakest bond. Our goal is to find out whether there is a correlation between the westest bond strength of a high explosive molecule and its impact sensitivity

CALCULATIONAL DETAILS

All total energy calculations were performed using the Gaussian 94/DFT package with spin-polarized gradient-corrected exchange and correlation functionals. In the calculations of RDX

decomposition, we have chosen four widely adopted and promising functionals: B-PW91, B3-PW91, B-LYP and B3-LYP. B refers to the Becke's 1988 gradient-corrected exchange functional which reproduces the exact asymptotic behavior of exchange-energy density in finite system, and B3 is denoted for the Becke's hydrid method of mixing Hartree-Fock exchange energy into the exchange functional. PW91 and LYP are the gradient-corrected correlation functionals of Perdew-Wang, and Lee, Yang and Parr. Three Gaussian-type basis sets were used for the Kohn-Sham orbital expansion: Dunning's valence double zeta (D95V), D95V plus diffuse function (D95V+), and Dunning's most recent correlation consistent polarized valence double zeta basis sets (cc-pVDZ).

In the comparative study of bond dissociation energies of a series of high explosives, we have used the D95V basis set and the B-PW91 funcitonal, as we found them to give the correct trend for bond dissociation energies of RDX. Zero point energy corrections were not included, since we do not expect those small energy corrections to effect the qualitative results.

RESULTS AND DISCUSSIONS

A. RDX Decomposition Mechanism.

The results for the $N\text{-}NO_2$ bond dissociation energy (D) are presented in Table 1. D_e and D_0 refer to the values without and with zero point correction of the vibrational energy, respectively, which was calculated at the B-PW91/D95V level. It is satisfying to see that the four functionals we used give consistent results. Although adding polarization functions has a larger effect than adding diffuse functions, neither changes the value of D significantly. For instance, the largest deviation between D95V and D95V+ is -0.9 kcal/mol (B-LYP), while that between D95V and cc-pVDZ is -2.9 kcal/mol (B-PW91). The deviation between the basis sets considered is roughly the same as the deviation between the functionals. Becke's hydrid B3 method gives a slightly higher value of the bond energy (about 4 kcal/mol) than Becke 88. Using our largest basis set (cc-pVDZ), four functionals give D_e ranging from 38.7 to 43.3 kcal/mol, with an average value of 41.0 kcal/mol and the maximum deviation of ± 2.3 kcal/mol. Taking the zero point energy correction into account, we predict that the $N\text{-}NO_2$ bond energy D_0 is 34.2 kcal/mol at the B-PW91/cc-pVDZ level.

Table 1. Acronyms and abbreviations used for high explosive materials.

DATB	**Diaminotrinitrobenzene**
Dingu	**Dinitroglycourile**
Edna	**Ethylenedinitramine**
HMX	**Octahydro-1,3,5,7-tetranitro-1,3,5,7 tetraazacine**
HNB	**Hexanitrobenzene**
NG	**Nitroglycerine**
NTO	**3-nitro-1,2,4-triazol-5-one**
PETN	**Pentaerythritol tetranitrate**
RDX	**Hexahydro-1,3,5-trinitro-1,3,5 -triazine**
TATB	**Triaminotrinitrobenzene**
TETRYL	**N-methyl-N,2,4,6-tetranitro Benzeneamine**
TNA	**Trinitroaniline**
TNAZ	**Trinitroazetidine**
TNB	**2,4,6-trinitrobenzene**
TNT	**2,4,6-trinitrotoluene**

Our DFT values of the $N\text{-}NO_2$ bond energy in RDX are significantly smaller than the previous estimate of 48 kcal/mol, which was based on the assumption that the $N\text{-}NO_2$ bond in RDX is similar to that of methyl-nitramine and nitramine. We have performed the same level of calculations on methyl-nitramine and nitramine and found that RDX has a weaker $N\text{-}NO_2$ bond than nitramine and methyl-nitramine due to both geometric and electronic relaxations through the RDX

ring fragment ($H_6C_3N_5O_4$).. Our estimate for the RDX geometric stabilization is between 2-6 kcal/mol. Electronic relaxation is thus the dominant mechanism; it accounts for 6-10 kcal/mol.

Table 2. Calculated RDX N-NO_2 Bond Dissociation Energy (D) and Heat of Reaction (ΔE) for RDX Ring Fission Dissociation Pathway.

Calculation	D_e (D_o)	ΔE_e (ΔE_o)
B-PW91/D95V	41.6(37.1)	63.7(54.5)
B-PW91/D95V+	41.2(36.7)	59.5(50.3)
B-PW91/cc-pVDZ	38.7(34.2)	51.0(41.8)
B-LYP/ D95V	42.1(37.6)	51.3(42.1)
B-LYP/ D95V+	41.2(36.7)	48.9(39.7)
B-LYP/ cc-pVDZ	39.5(35.0)	45.5(36.3)
B3-PW91/D95V	43.6(39.1)	77.8(68.6)
B3-PW91/D95V+	44.3(39.8)	74.9(65.7)
B3-PW91/cc-pVDZ	43.3(38.8)	66.0(56.8)
B3-LYP/ D95V	42.4(37.9)	69.1(59.9)
B3-LYP/ D95V+	41.9(37.4)	64.3(55.1)
B3-LYP/ cc-pVDZ	42.5(38.0)	58.3(49.1)

The adiabatic potential energy curve of breaking of N-NO_2 bond (shown in Figure 1) was obtained by optimizing the geometry at each fixed N-NO_2 separation at the B-PW91/D95V level. We found the potential energy profile has zero barrier (the typical case for a radical recombination reaction). This is in agreement with the experimental observation that the product translational energy distribution for N-NO_2 bond rupture is peaked at zero. Therefore, the barrier for breaking the N-NO_2 bond is approximately equal to N-NO_2 bond energy D_o.

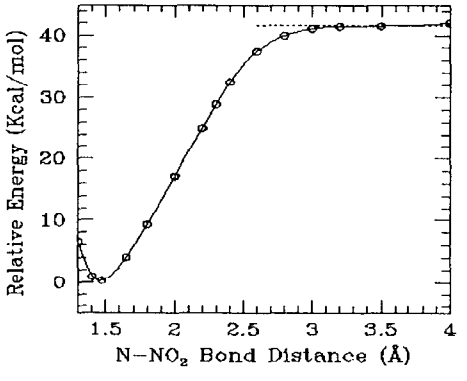

Figure 1. Potential Energy Curve of RDX Dissociation via N-NO_2 Bond Rapture Along the Reaction Coordinate (N-NO_2 bond).

The heat of reaction (ΔE) for the concerted symmetric ring fission II is also listed in Table I. It was calculated in the same fashion as the N-NO_2 bond dissociation energy. Note that the deviation between various exchange-correlation functionals and basis sets are larger than for pathway I. This perhaps is due to the large change in the electronic character from RDX to H_2CNNO_2. However, this pathway involves rearrangement of three chemical bonds. If one estimates the deviations between functionals and basis sets based on the unit of changing bond, they are not too far from those of pathway I. For instance, Becke's hybrid method (B3) again gives consistently higher values (about 5 kcal/mol per bond) than Becke 88. Nevertheless, the heat of reaction for the ring fission is systematically higher than the N-NO_2 bond dissociation energy within the same functional and basis set. Using the largest basis set cc-pVDZ, four functionals give ΔE ranging from 66.0 to 45.5 kcal/mol, with an average value of 55.2 and maximum deviation of ±10.2 kcal/mol. Taking the zero point energy correction of 9.2 kcal/mol, our best estimate for the heat of reaction of the concerted ring fission is at the B-PW91/cc-pVDZ level is 41.8 kcal/mol.

We then mapped the potential energy profile of the ring fission (see Figure 2) in order to identify the transition state. The reaction coordinate parameter β is chosen to be the three alternate C-N distances along the breaking C-N bonds (indicated as the dashed line
in Figure 2). At each β, we optimized all other degrees of freedom at both B-PW91/D95V and B-PW91/D95V+ level. Although adding diffuse functions lowers the potential energy, the energy profiles of the D95V and D95V+ basis sets have a similar shape, including the same β of 2.21Å at the saddle point. We have assumed that cc-pVDZ has the same β value for the saddle point, therefore the transition state at cc-pVDZ level is obtained by optimizing all other degree of freedoms while keeping β at 2.21Å. This B-PW91/cc-pVDZ calculation gives a transition state height of 58.1 kcal/mol. The Hessian calculation at the B-PW91/D95V level shows one imaginary frequency for the predicted transition state. Taking into account the zero point energy correction, our best estimate of barrier height at B-PW91/cc-pVDZ level for pathway II is 52.5 kcal/mol. Note that this value is about 20 kcal/mol smaller than the previous LDA result.

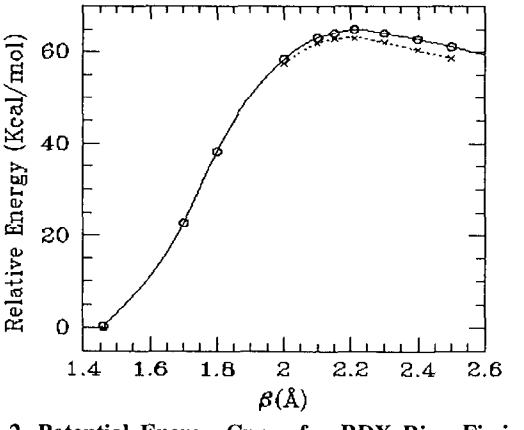

Figure 2. Potential Energy Curve for RDX Ring Fission Reaction Along
the Reaction Coordinate (theBbroken C-N Bond, β).

A detailed comparison between path I and path II requires the evaluation of not only the barriers, but also the reaction prefactors. Using a simple kinetic and transition state theory, we estimated the prefactors to be $7x10^{17}$ s^{-1} and $1x10^{17}$ s^{-1} for

channel I and II, respectively. Since the prefactors for path I and II are of the same order of magnitude, we predict path I to be the dominant channel due to its lower activation barrier.

In conclusion, we have found that the activation barrier for concerted ring fission is roughly 18 kcal/mol greater than that for N-NO_2 bond rupture, a difference that is significantly larger than the maximum deviation found between different functionals. This suggests that thermal gas phase decomposition at temperatures significantly under 18 kcal/mol (about 9000K) most likely proceeds via N-NO_2 bond rupture. In addition, simple kinetic and transition state theory calculations indicate that the prefactors for these two paths differ very little, thus they do not play a significant role in differentiating the rates. Although more sophisticated kinetic rate theories such as variational transition state theory and anharmonicity may change the prefactor by a factor of 6 or greater, the uncertainties in our estimated prefactors are small compared to the difference in barrier heights at temperatures of interest. Thus, our results suggest that path I is the dominant channel in gas phase thermal RDX decomposition.

B. Comparative Study of Bond Dissociation Energies in High Explosives

DFT bond dissociation energies of the nitrated aromatic benzene rings: TATB, DATB, TNA, TNB, TNT and HNB are displayed in Table 2 to 7. We found C-NO_2 is the weakest bond for all molecules in this group. As we expected, having NH_2 adjacent to NO_2 increases the stability of C-NO_2 bond due to hydrogen bonding between NH_2 and NO_2. For instance, the weakest C-NO_2 bond strength of TNB, TNA, DATB and TATB increases from 67.7, 71.6, 74.6 to 77.2 as number of NH_2 increases from 0, 1, 2 to 3, respectively. The strength of NO_2-NH_2 hydrogen bonding is estimated to be in the order of 2-4 kcal/mol. The hyrogen bond lengths for this group of molecules are also in the typical range. For TATB, the distance between O of NO_2 and H of the adjacent NH_2 is 1.691 A.

The second weakest bonds for TATB, TNA and DATB are the C-NH_2 bonds, which varies slighly from 124.1, 128.8 to 131.1 kcal/mol, respectively. Note that the C-NH_2 groups of TATB, TNA and DATB have identical nearest neighbors indicating the localized nature of the C-NH_2 bonding. C-NH_2 bond strengths are significantly (about 50 kcal/mol) stronger than those of C-NO_2 due to the electronic relaxation of NO_2 fragment. The difference between C-NO_2 and C-NH_2 bond strengths is also reflected in the C-N separations (R). For instance, R(C-NH_2) of TATB is 0.095 A shorter than R(C-NO_2) of 1.446 A. Within this group, the values of R(C-NO_2) and R(C-NH_2) do not vary significantly.

C-H (C is a ring Carbon) bond are the strongest bonds for this group of high explosive molecules. Note that C-H bond strengths of TNA, MATB, TNB and TNT are similar (154.3, 152.9, 152.0, 151.9 kcal/mol, respectively) as they have a similar local bonding environments. In comparison, the C-H bond from the CH_3 group of TNT is about 30 kcal/mol weaker than those of C(ring)-Hs. This difference reflects the fact that sp^2 C forms a stronger bond with H than sp^3 C.

For TATB, DATB, TNA, TNB and TNT, we found that the NO_2, NH_2 funtional groups on the six-carbon ring lay in almost the same plane as the ring. The planar arrangement promotes the hydrogen bonding between NO_2 and NH_2 and the electron conjugation effect between NO2 and the benzene ring. It costs 18 kcal/mol to rotate three NO_2 groups of TNB 90 degrees from its planar position to be perpendicular to the ring, from which we estimated the conjugation effect to be roughly 6 kcal/mol per NO_2. For HNB, which has six NO_2 groups, intramolecular repulsions between the NO2 groups prevents a planar geometry. We found that the lowest energy structure has alternating in plane and out of plane NO_2 groups. This structure is 0.6 kcal/mol lower in energy than the structure of six NO_2 all being perpendicular to the ring. In Table 7, we listed the bond energy of C-NO_2 for the three NO_2 groups that are perpendicular to the plane. In comparision, the C-NO_2 bonds where the NO_2 groups are in plane are 4.7 kcal/mol stronger, which is consistent with the electron conjugation effect of 6 kcal/mol per NO_2 estimated from TNB.

The results for HMX and TNAZ are listed in Table 8 and 9, respectively. The N-NO_2 bond strength of HMX was calculated to be 42.8 kcal/mol at the BPW91/D95V level, which is similar to that of RDX (41.6 kcal/mol at the same level of calculation). For TNAZ, we have found that the N-NO_2 is stronger than the C-NO_2 bond by about 3 kcal/mol, in contrast to an observation that the C-NO_2 bond is typically stronger than N-NO_2 bond.

CONCLUSION

We have listed the calculated (BPW91/D95V level) bond strengths of the weakest bond (N-NO_2 or C-NO_2) and sensitivities for not only compounds mentioned above, but also NTO, EDNA, DINGU, PETN and Nitroglycerin in Table 10.The impact and friction sensitivity measurement is taken from reference by Kohler and Meyer. Notes that these types of measurement are typically rough. For instance, the reported friction sensitivity cannot distinguish the sensitivity difference between TATB, TNA, TNB and TNT. In a larger sensitivity scale the bond strength of the weakest bond correlates well with the sensitivity measurement. A calculation of the bond dissociation energy should provide a useful rough estimate of the sensitivity of the explosive. Other properties, such as energy content, explosive morphology, particle size, and defect concentration should be taken into account when considering the sensitivity of high explosive molecules.

TABLE 4. DFT BOND DISSOCIATION ENERGIES (D) AND BOND LENGTHES (R) IN TATB.

Decomposition Pathways	BPW91/D95V
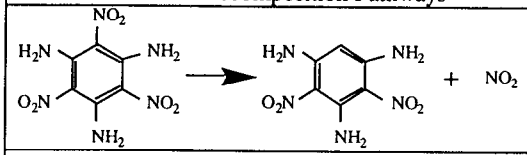	$D(C\text{-}NO_2)$ = 77.2 kcal/mol $R(C\text{-}NO_2)$ = 1.446 Å
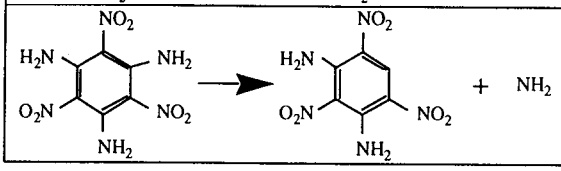	$D(C\text{-}NH_2)$ = 124.1 Kcal/mol $R(C\text{-}NH_2)$ = 1.351 Å

TABLE 5. DFT BOND DISSOCIATION ENERGIES (D) AND BOND LENGTHES (R) IN DATB.

Decomposition Pathways	BPW91/D95V
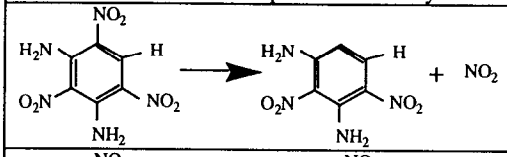	$D(C\text{-}NO_2)$ = 74.6 Kcal/mol $R(C\text{-}NO_2)$ = 1.469 Å
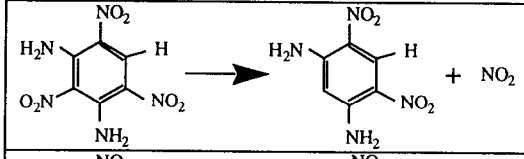	$D(C\text{-}NO_2)$ = 76.1 Kcal/mol $R(C\text{-}NO_2)$ = 1.451 Å
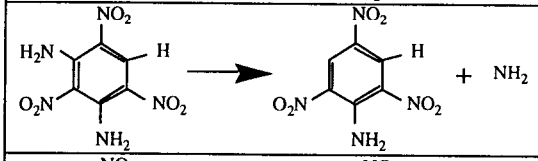	$D(C\text{-}NH_2)$ = 128.8 Kcal/mol $R(C\text{-}NH_2)$ = 1.351 Å
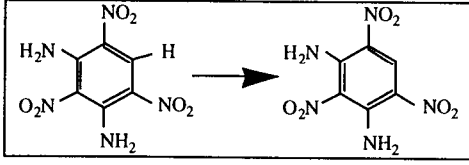	D(C-H) = 152.0 Kcal/mol R(C-H) = 1.092 Å

TABLE 6. DFT BOND DISSOCIATION ENERGY (D) AND BOND LENGTHS IN TNA.

Decomposition Pathways	BPW91/D95V
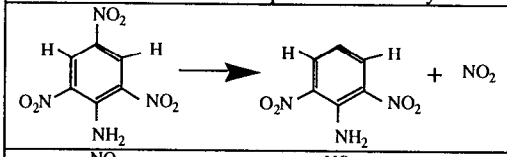	$D(C\text{-}NO_2)$ = 71.6 $R(C\text{-}NO_2)$ = 1.481 Å
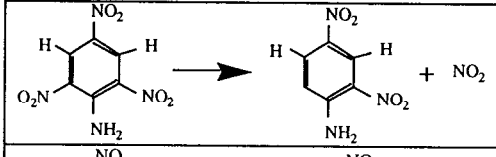	$D(C\text{-}NO_2)$ = 71.1 K $R(C\text{-}NO_2)$ = 1.478 Å
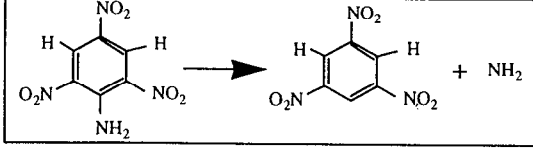	$D(C\text{-}NH_2)$ = 131.0 K $R(C\text{-}NH_2)$ = 1.353 Å

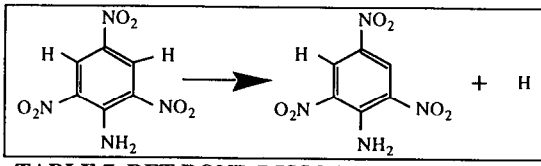	D(C-H) = 152.9 Kcal/mol R(C-H) = 1.092 Å

TABLE 7. DFT BOND DISSOCIATION ENERGIES (D) AND BOND LENGTHES (R) IN TNB.

Decomposition Pathways	BPW91/D95V
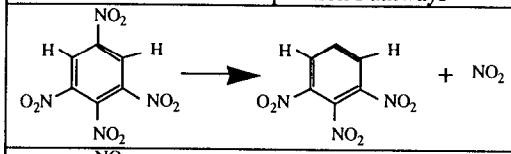	D(C-NO_2) = 67.7 Kcal/mol R(C-NO_2) = 1.498 Å
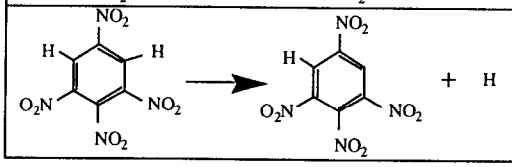	D(C-H) = 154.3 Kcal/mol R(C-H) = 1.091 Å

TABLE 8. DFT BOND DISSOCIATION ENERGIES (D) AND BOND LENGTHES (R) IN TNT.

Decomposition Pathways	BPW91/D95V
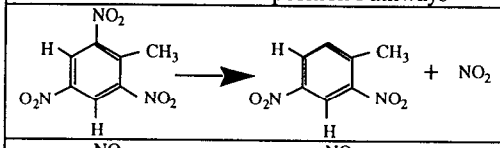	D(C-NO_2) = 62.4 Kcal/mol R(C-NO_2) = 1.512 Å
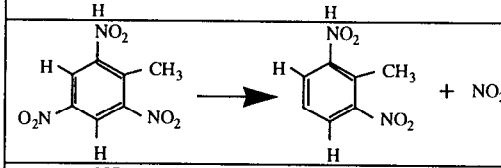	D(C-NO_2) = 67.0 Kcal/mol R(C-NO_2) = 1.492 Å
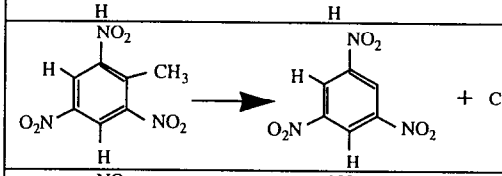	D(C-CH_3) = 102.3 Kcal/mol R(C-CH_3) = 1.514 Å
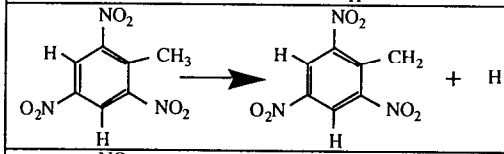	D(C-H) = 123.8 Kcal/mol R(C-H) = 1.107Å
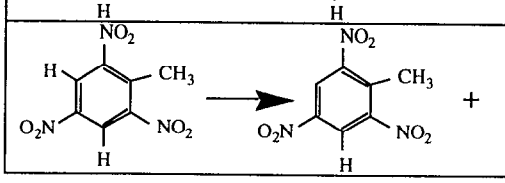	D(C-H) = 151.3 Kcal/mol R(C-H) = 1.091 Å

TABLE 9. DFT BOND DISSOCIATION ENERGIES (D) AND BOND LENGTHES (R) IN HNB.

Decomposition Pathways	BPW91/D95V
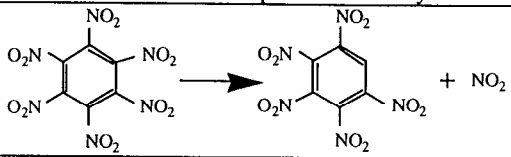	D(C-NO_2) = 43.8 kcal/mol R(C-NO_2) = 1.518Å

TABLE 10 DFT BOND DISSOCIATION ENERGIES (D) OF HMX.

Decomposition Reaction	BPW91/D95V
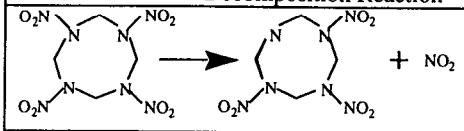	$D(N\text{-}NO_2)$ = 42.8 kcal/mol $R(N\text{-}NO_2)$ = 1.422Å

TABLE 11. DFT BOND DISSOCIATION ENERGIES (D) OF TNAZ.

Decomposition Reaction	BPW91/D95V
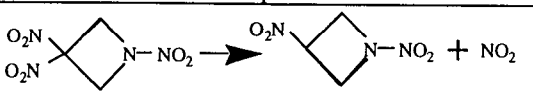	$D(C\text{-}NO_2)$ = 39.8 kcal/mol $R(C\text{-}NO_2)$ = 1.560Å
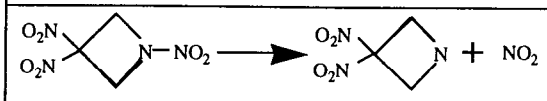	$D(N\text{-}NO_2)$ = 43.9 kcal/mol $R(N\text{-}NO_2)$ = 1.424Å

TABLE 12. BOND STRENGTH (KCAL/MOL) OF THE WEAKEST BOND AND IMPACT/FRICTION SENSITIVITY OF HIGH EXPLOSIVES.

HE	Weakest Bond	De	Impact (Nm)/ Friction (N) Sensitivity
TATB	C-NO_2	77.2	50/353
DATB	C-NO_2	74.6	3.20m
TNA	C-NO_2	71.6	15/353
NTO	C-NO_2	67.8	>280cm
TNB	C-NO_2	67.7	7.4/353
TNT	C-NO_2	62.4	15/353
EDNA	N-NO_2	49.4	8
HNB	C-NO_2	43.8	
DINGU	N-NO_2	43.1	5-6
HMX	N-NO_2	42.8	7.4/120
RDX	N-NO_2	41.6	7.5/120
TNAZ	C-NO_2	39.8	
PETN	O-NO_2	39.8	3/60
NG	N-NO_2	37.6	0.2/
Tetryl	N-NO2	28.7	3/353

ACKNOWLEDGMENT

This work was performed under the auspices of the U. S. Department of Energy by the Lawrence Livermore National Laboratory under contract No. W--7405--ENG--48.

---

[1] Wight C.A. and Botcher T. R., J. Am. Chem. Soc., **114**, 8303 (1992).